EFFECTS OF THE MOTOR ON THE STABILITY OF A SINGLE AXIS CONTROLLED MAGNETIC BEARING

Fernando Antonio Camargo, camargoF@usp.br

Oswaldo Horikawa, ohorikaw@usp.br
Escola Politécnica of São Paulo University, EPUSP-PMR, Av. Prof. Mello Moraes, 2231, 05508-900, SP Brazil

Isaias da Silva, isaias.silva@unifesp.br
Federal University of São Paulo, Dep. of Exact Sciences and Earth, R. Prof. Artur Riedel, 720, 09972-270, Diadema, SP, Brazil

Orlando Homen de Mello, orlandoh@usp.br

José Roberto Cardoso, cardoso@pea.usp.br
Escola Politécnica of São Paulo University, EPUSP-PMR, Av. Prof. Mello Moraes, 2231, 05508-900, SP Brazil

Abstract. This work is part of the development of an implantable Ventricular Assist Device (VAD) in which the pump rotor is suspended by a single degree of freedom (1-DOF) magnetic suspension. In order to drive de DAV's rotor, two brushless BLDC motor types, axial and radial architectures, have been developed and tested in a magnetic bearing prototype with active control only in 1-DOF of the rotor, i.e., its axial direction. In such bearing architecture, radial and angular stability are assured by a constant and positive magnetic stiffness between two pairs of permanent magnets working in attraction mode and placed in each end of the bearing's rotor. Therefore, the BLDC motor applied to the bearing can cause rotor instability mainly along its passive directions, i.e. axial and radial, and also along its axial direction, e.g. if the axial electromagnetic actuators are overloaded by the magnetic forces produced by the motor. So, this paper presents some of the brushless motors development stages and several experimental results, conducted with the axial and radial motors architectures applied to the magnetic bearing, are also shown which demonstrate the viability of the proposal.

Keywords: magnetic bearing, bearingless motor, brushless DC motor, magnetic suspension, magnetic bearing.

1. INTRODUCTION

The Escola Politécnica of São Paulo University (EPUSP) and the Institute Dante Pazzanese of Cardiology (IDPC) are conducting a joint project aiming the development of an implantable Ventricular Assist Device (VAD). Based on a VAD of external use, developed previously by the IDPC (Andrade et al, 1996), the new VAD will use a magnetic bearing to suspend the rotor without any mechanical contact of the rotor and other VAD components. With respect to the new VAD, authors already reported results of preliminary studies (Horikawa *et al*, 2008). The magnetic bearing architecture that will be used in the VAD under development is of a type presented at Silva and Horikawa (2000) in which, the active control is executed only along the axial direction of a rotor (Fig.1). At each extremity of the rotor, a permanent magnet is fixed. Facing each of these magnets, another magnet is fixed to one base so as to have an attraction force between each pairs of magnets which assures radial and tilting stability of the bearing rotor. As each pair of magnets works in attraction mode, the rotor axial direction is unstable. So, along the axial direction, the rotor stability is assured by a control system composed by a non-contact sensor, a controller, an amplifier and two actuators. In this work this bearing is referred as AMB-EPUSP. This bearing is elected mainly because of its simplicity in terms of mechanical configuration and in terms of control system: important factors to increase the reliability of the bearing intended to be used in an implantable VAD.

Figure 2 shows one possible configuration for the VAD that adapts the AMB-EPUSP, shown in Fig.1, to the VAD-IDPC. Two electromagnetic actuators with ferromagnetic core are placed at the upper and lower extremities of the rotor. At the top surface of the lower actuator a coil is set so as to work as a probe of a non-contacting inductive gap sensor. At both extremities of the rotor cylindrical rare earth (NdFeB) permanent magnets are fixed. The attraction forces between these magnets and the ferromagnetic core confine the rotor in a central position. The axial position of the rotor is actively controlled in the same fashion as described before. Thus, by applying the AMB-EPUSP the problem of the levitation of the VAD rotor is being solved. Now the project faces the problem of driving the rotor so as to pump the blood.

Considering aspects such as reliability, efficiency and small dimensions to realize an implantable VAD, the BLDC electric motor type naturally arises as the best solution for driving the rotor, instead of other electric motor types. Strictly speaking, a brushless DC (BLDC) motor is elected due to the same reason a magnetic bearing is choose, i.e., the motor should not contact the rotor, minimizing problems of damage to the blood components. However, the magnetic forces that drive of the rotor may interfere in the magnetic suspension causing rotor instability. As described at Silva and Horikawa (2000), the rotor is stable with respect to all degrees of freedom excepting for its axial position. In the AMB-EPUSP, the distance between magnets at the extremities of the rotor must be larger than the diameter of these

magnets. Otherwise the rotor inclines and loses its tilting stability. Therefore it is reasonable to expect that the BLDC motor will interfere in the magnetic suspension. As a first step in the study to investigate these interference, in this work, two type of BLDC motor is developed and used to drive a rotor suspended by the AMB-EPUSP: axial motor (Fig.3(a)) and radial motor (Fig.3(b)).
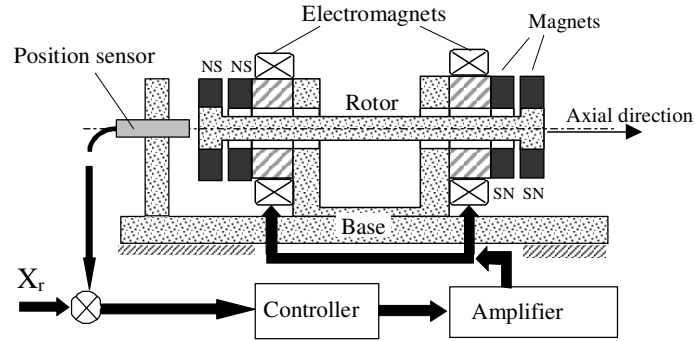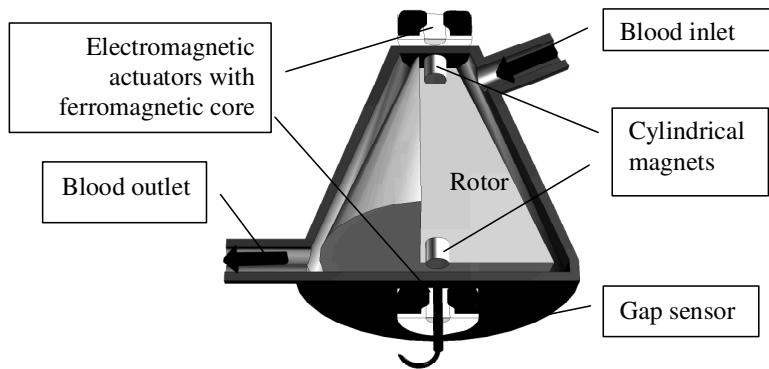

Figure 1. The magnetic suspension AMB-EPUSP

Figure 2. DAV-IDPC with EPUSP magnetic bearing
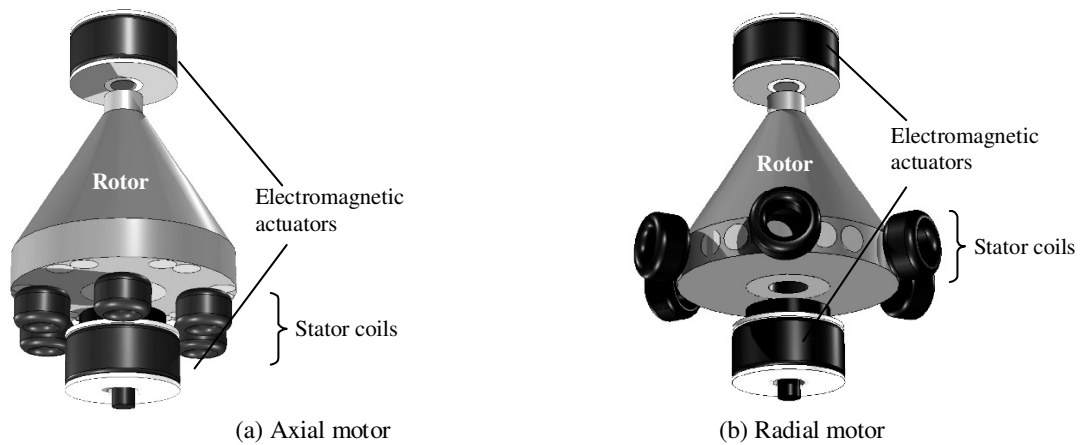

(a) Axial motor

(b) Radial motor

Figure 3. Evaluated BLDC motors for the DAV-IDPC rotor

Next sections will describe all steps executed, up to now, to allow the final tests: (i) design, construction and testing of the axial and the radial BLDC motors; (ii) design, construction and testing of AMB-EPUSP and the rotor to be driven

be both BLDC motors and (iii) estimate the BLDC motors behavior using FEM analysis. The final experimental tests execution aimed to identify how each motor assemble option interacts with the AMB-EPUSP has not been concluded yet.

2. BLDC MOTOR DESIGN

On designing the BLDC motor used on the tests, a coreless configuration is adopted. This eliminates any undesired magnetic forces among the rotor, the permanent magnets and the stator iron core. The coreless BLDC had been used by Asama *et al* (2004) to improve his motor balance and to save energy, i.e., the magnetic forces produced by the motor do not affect the magnetic bearings. This approach has been corroborated by the Ooshima (2007) analysis, pointing that the rotor torque was not affected by the presence, or absence, of any ferromagnetic material on the rotor. The absence of any ferromagnetic material on the stator core eliminates the cogging torque while improves the motor power density reducing the motor weight (Aboulnaga e Emadi, 2004).

A suitable VAD' BLDC motor must be able to pump 5 liters of blood per minute at 100 mmHg, with the rotor at 2000 RPM (Asama *et al*, 2004; Legendre *et al*, 2008; de Berne and Levy, 2001). To achieve these values the motor must provide a minimum torque of 0.013 Nm and a minimum mechanical power of 2.8W.

Figure 4 shows the special shape rare earth (NdFeB) permanent magnet used in the BLDC motor rotor, axial and radial types. The rotor uses 3 pairs of this magnet while the coreless stator windings has been designed with three phases, each phase with six coils and each coil with 22 turns of AWG 27 copper wire. The BLDC motor has been powered by a commercial controller (PICDEM MC LV, Microchip) using a sensorless algorithm.

Figure 4. Permanent magnet used on the BLDC motor rotor

In order to evaluate the BLDC motor main characteristics its rotor was assembled in a mechanical axis and connected to a dynamometer. The axial motor was able to provide 0.014 Nm of maximum torque at 3072 RPM and 4.8 W of maximum mechanical power at 3924 RPM. On the other hand the radial motor was capable to provide 0.017 Nm of maximum torque at 2294 RPM and 5.3 W of maximum mechanical power at 4063 RPM. Therefore, both motors architectures present the required VAD motor characteristics.

3. MAGNETIC SUSPENSION DESIGN

As the AMB-EPUSP main characteristics are dependent of the magnetic actuator and of the permanent magnets on the rotor, the designed magnetic suspension must be analyzed to observe what changes each BLDC motors architecture causes in the magnetic suspension stability. Figure 5 shows the set-up used for initial testing of the magnetic suspension. Here, the rotor is driven by compressed air blown to the rotor periphery. An external coil and an oscilloscope are used to measure the rotor speed.

Figure 5. Set-up for testing the magnetic suspension.

There are three elements that may directly affect the efficiency of this magnetic suspension (Silva, 2005): (i) the actuator electromagnetic constant k_t (the ratio of the current furnished to the actuator and to the force generated by the actuator,) and the actuator magnetic constant k_h (the ratio of the gap between the magnetic pair and to the generated magnetic force,). To improve these values the rotor weight was minimized to a final value of 0.98 N (to improve the axial stiffness) and the rotor height was reduced to 84.6 mm (to improve the angular stiffness). Moreover, a gap sensor was designed in order to maximize sensor accuracy.

On the final assemble the rotor has been magnetically suspended with 6.8 mm of total gap (upper gap plus lower gap). The magnetic suspension experimental tests gave the following values: electromagnetic constant of 2.2 N/A and a magnetic constant of 2.5 N/mm.

Also, during the magnetic suspension experimental tests two major problems were identified and have impacted the tests with the two BLDC motors options. First, a problem of unbalanced rotation was verified. This unbalanced was not caused by rotor mass unequal distribution but by the non-uniformity in the magnetization of the magnets. In both magnets fixed to the rotor their magnetization center did not coincide with their geometric center. Due to this problem, the rotor presented radial oscillations even at very low speeds (amplitude oscillations larger than 2 mm in radial direction). This problem was solved by selecting magnets with uniform magnetization.

The second problem was detected during rotation tests when compressed air was blown to the rotor periphery and higher speed was reached. When the rotation speed reached speeds between 860 and 1000 RPM, the rotor vibrated laterally with amplitudes of a few millimeters. Despite these rotor lateral oscillations, the radial stiffness of the magnetic suspension was sufficient to keep the rotor stable and avoiding its collision with the bearing walls. However, at higher speeds, near 2000 RPM, the rotor lateral vibrations changed suddenly to angular vibrations and cause the rotor to collide to the bearing wall.

These rotor dynamic resonance problems observed here were similar to the Silva (2005) test problem description. To avoid these problems all tests with the two BLDC motor options were done with speeds not higher than 600 RPM. Wherever, this lower speed will not invalidate the motor tests.

4. THE BLDC MOTOR FEM ANALYSIS

With the behavior of the magnetic suspension identified and the BLDC motor being operational, both units have been integrated to evaluate the magnetic interaction between them. Before start the experimental tests and aiming to estimate some motor characteristics, each BLDC motor option had been analyzed using a finite element method (FEM) tool. These numerical analyses have been used to identify how forces on the rotor are affected when some external force changes the rotor position. On a regular VAD, the external force should be generated by the heart beating or some patient movement.

4.1 The Axial BLDC Motor

Figure 6 illustrates the FEM model used to analyze the axial BLDC motor architecture. Using this simplified model, the forces acting on the rotor could be estimated considering different rotor angle (around z axis) and different winding currents. The analysis is done considering rotor specific displacement and evaluating if the windings induce any new force on the rotor, excepting torque. The generated force amplitude and its direction are analyzed to determine if it should be a problem or not. Fig.7 shows the three types of magnetic interference that the axial motor may cause on the suspended rotor: (a) axial displacement, (b) angular displacement, and (c) radial displacement.
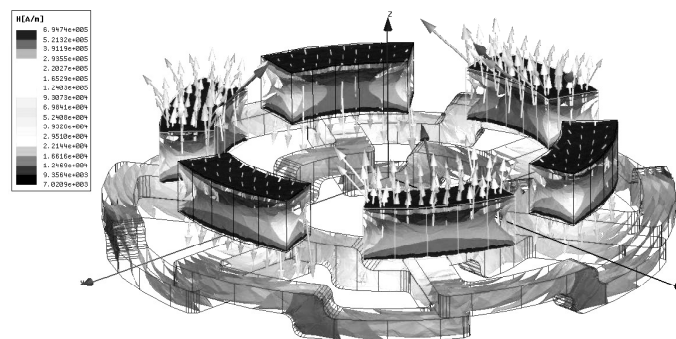

Figure 6. FEM analysis of the axial BLDC motor architecture.

Figure 7(a) illustrates the moving effect of axial displacement on the rotor. The force generated by the axial displacement had been analyzed to check if it creates a positive retro feeding or not. Fig. 8 shows the axial force induced on the rotor, while the rotor is rotating, for different values of gap.

The axial force curves show that the force is inversely proportional to the gap, i.e., as smaller is the rotor gap as higher is the axial force induced on the rotor by the axial stator. All force curves resemble a saw tooth shape and has a base frequency that is 18 times (since the motor is 6 poles times 3 phases) higher than the rotor speed. It is important to observe that the magnetic bearing active control must directly compensate this axial force.

(a) Axial
displacement

(b) Tilting
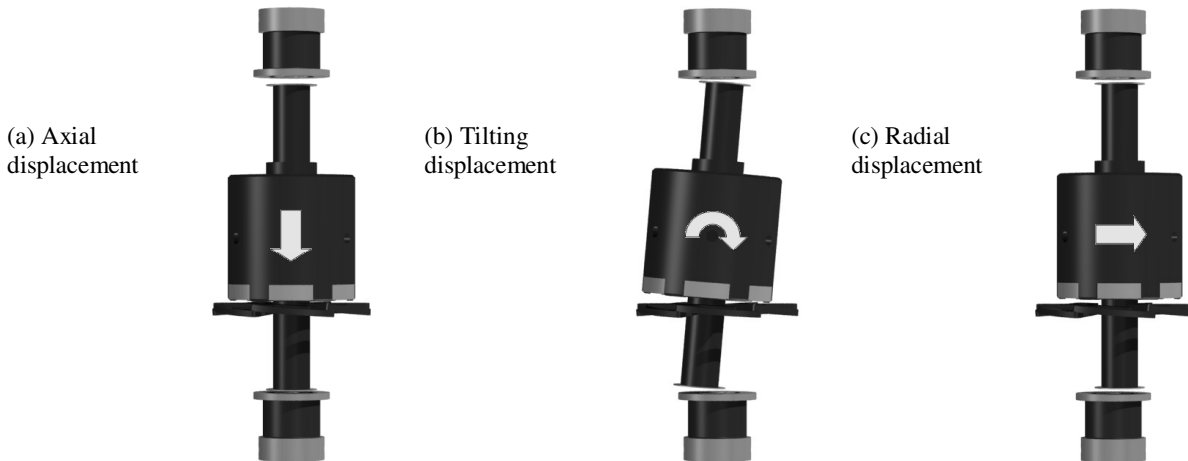displacement

(c) Radial
displacement

Figure 7. Draft of the axial BLDC motor architecture assembled to a 1-DOF magnetic bearing.
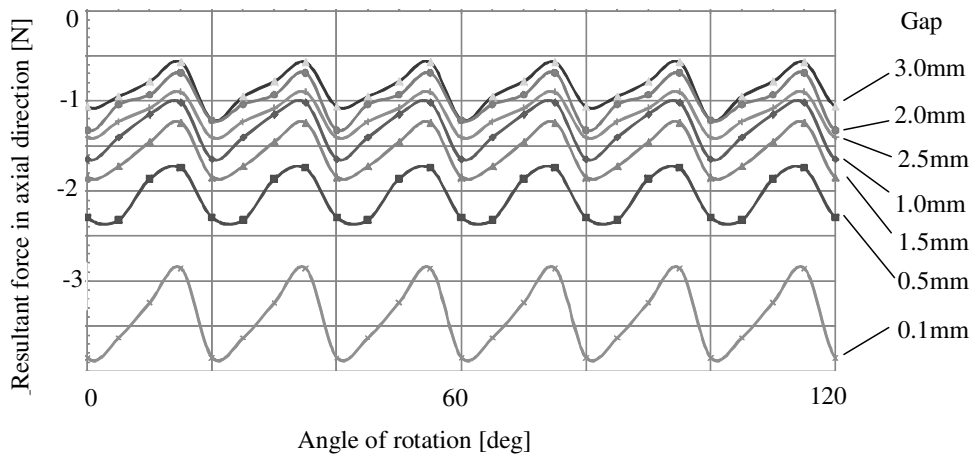

Figure 8. Results of the FEM analyses of the axial force versus rotor angular displacement and for several gaps produced by the axial BLDC motor architecture on the rotor.

Now, the FEM analyses are focused on how the axial force is affected by different amount of rotor tilting displacements (Fig.7(b)). Considering a default gap of 2 mm, the maximum tilting of ±2 degree of the rotor is considered. Fig. 9 shows how the maximum and minimum values of the force induced on the rotor in axial direction (saw tooth shape as shown in Fig. 8) change with the rotor tilting.. It is observed that on 0 degree of tilting, the force varies from −1.51 to −0.86 N). The same force varies from −1.29 to −0.71 N for a rotor tilting of −2 degree. As a general rule, the axial force varies with the inverse of the tilting amount, i.e., as higher is the rotor tilting as lower is the axial force induced on the rotor by the axial stator.

Finally, the FEM analyses are used to verify how the displacement of the rotor in the radial direction affects the axial force on the rotor. The analyses indicated that this effect is not significant, at least for radial displacements of ±2 mm.

After analyzing the effects of a variety of rotor displacements on the axial force, the torque generated by the axial motor is also analyzed by FEM. Fig. 10 shows a family of torque curves considering different winding current values from 0.5 A to 2 A. As higher is the current as higher is the torque. Fig. 10 also shows one example of the axial forces on the rotor to illustrate their relationship with the motor torque, e.g., the torque reaches a maximum value when the axial force reaches 50% of its peak value.
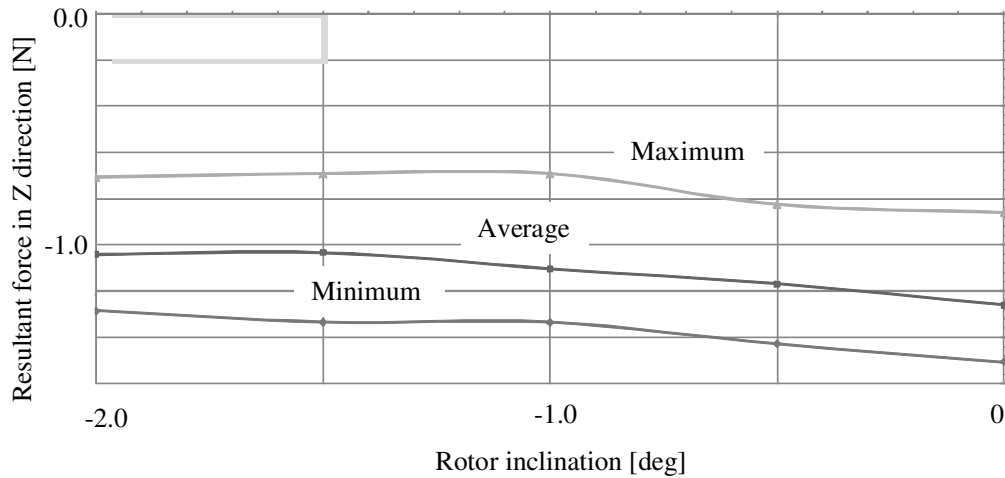

Figure 9. FEM analysis of the angular displacement on the axial BLDC motor
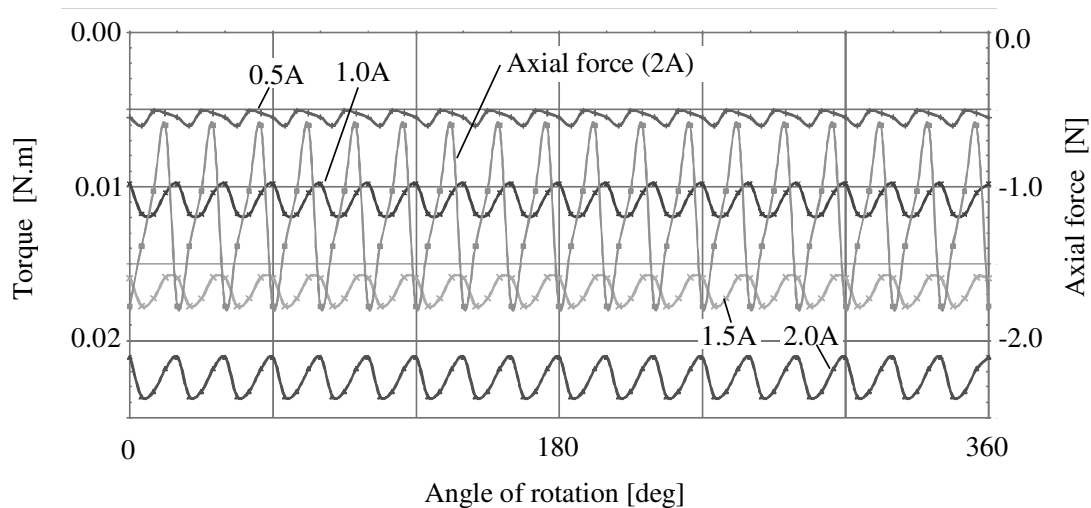

Figure 10. FEM analyses of the torque on the axial BLDC motor

4.2 The Radial BLDC Motor

Figure 11 illustrates the FEM model used in the analyses of the radial BLDC motor. Using this simplified model, the forces acting on the rotor can be estimated considering different rotation angle and different winding currents.

Similar to the analyses concerning axial motor, shown before, the analyses concerning radial motor is conducted considering rotor specific displacement and evaluating if the windings induce any new force on rotor, excepting torque. The generated force amplitude and direction was analyzed to determine if it should be a problem or not. Same displacements shown in Fig.7 are considered here.

The first FEM analyses considered effects of the axial displacements of the rotor (Fig.7(a)) on the axial force exerted by the stator on the rotor. Axial displacements in a range of ±2 mm are considered in the analyses. The second analysis considered effects of tilting displacements of the rotor (Fig.7(b)) in a range of ±2 degree, on the axial force. Finally, the third analysis considered the effect of radial displacements of the rotor (Fig.7(c)) in a range of ±2 mm on the axial force.
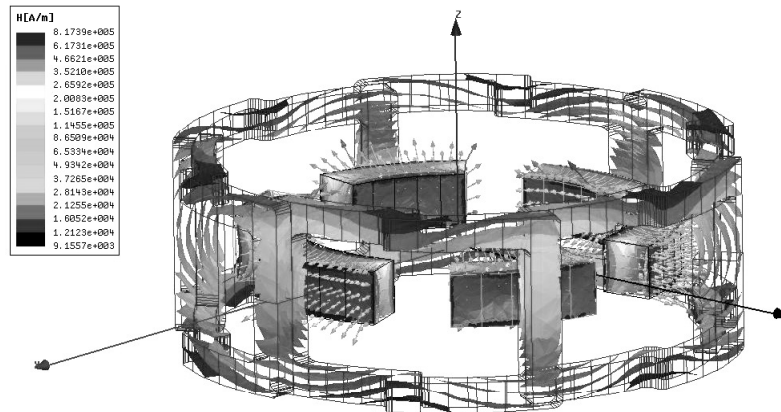
Figure 11. FEM analysis of the radial BLDC motor option

In any of the above analysis, no significant effect of the displacement on the axial force was observed. These results differ from those analytical results obtained in the axial motor. All efforts generated in the axial direction must be compensated by the AMB-EPUSP control system. Therefore, the absence of influence of the rotor displacements on the axial force makes the radial motor more favorable to be used with the AMB-EPUSP.

Besides the influence of rotor displacements on the axial force, the torque generated by the radial motor was also analyzed. Fig.12 shows a family of torque curves considering different current values in the coils, from 0.5 A to 2 A. As higher is the current, the higher is the torque. As in the axial motor, the torque curve oscillates with a frequency 18 times (since the motor has 6 poles and driven by 3 phases) higher than the rotor speed. However these oscillations do not impose limitations to the use of the AMB-EPUSP.
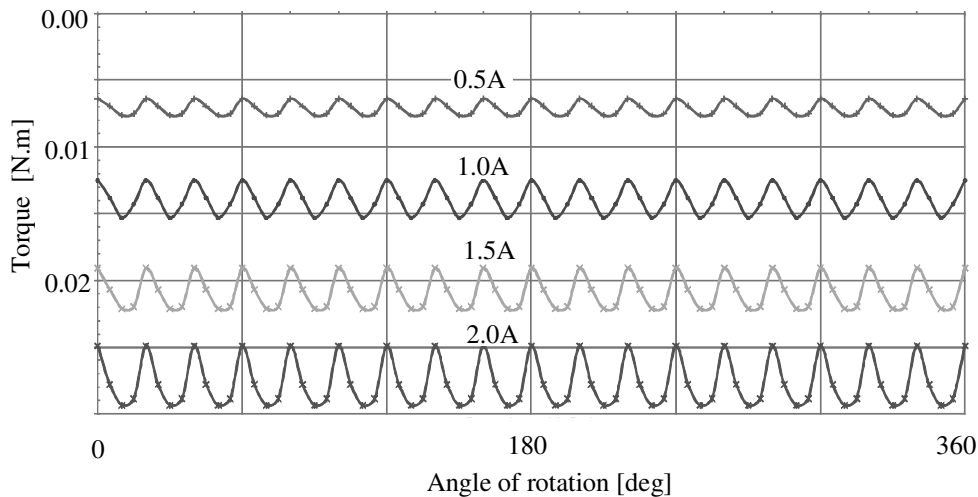

Figure 12. FEM analyses of the torque on the radial BLDC motor
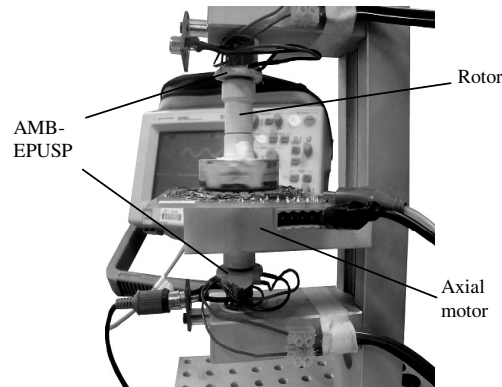
4.3 FEM Analysis Conclusion

The FEM analyses indicated that the radial BLDC motor as the preferable choice to drive the VAD with AMB-EPUSP, because the magnetic suspension does not need to compensate axial forces induced to the rotor by the motor stator.

All the forces induced on the rotor oscillate under a base frequency 18 times (since the motor is 6 poles times 3 phases) higher than the rotor speed. These force oscillation should be evaluate on the experimental tests phase to determine any influence on the magnetic suspension stability.
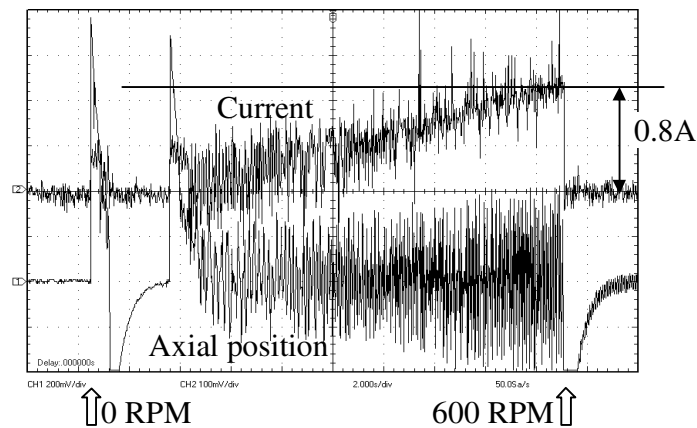
5. EXPERIMENTAL TEST

Due to the rotor dynamic problems detected on the magnetic suspension, all planned experiments with the BLDC motor options had to be changed. The original design was based on sensorless and required at least 2000 RPM to be become manageable, as no effort had been spent to improve the controller software. To operate at a lower speed, the BLDC motor controller firmware has been changed to accelerate from 0 to 600 RPM in 20 seconds before shutdown. Only the preliminary test results have been disclosure in this work.

Figure 13(a) shows the experimental set-up for tests with the axial BLDC motor. The tests have confirmed the FEM analyses, as the controller has to compensate the axial forces induced by the motor. Fig.13(b) shows how the current on the electromagnetic actuators increases from 0.02 to 0.8A while the motor speed changes from 0 to 600 RPM.
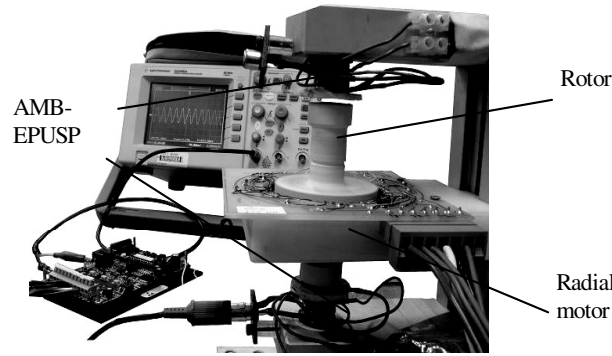

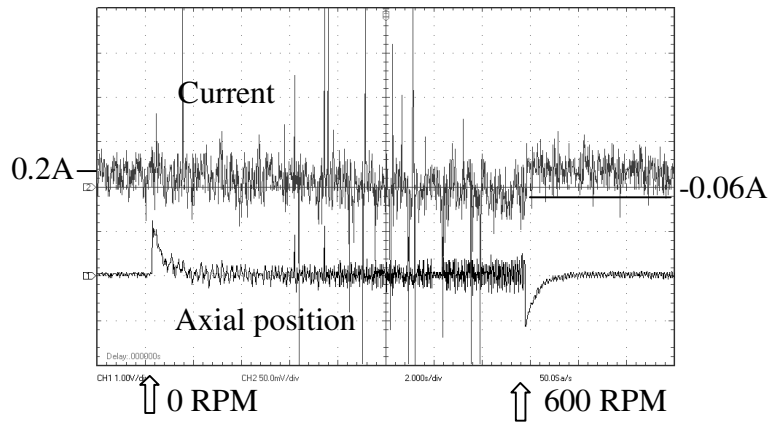(a)   Set-up

(b)   Current in the actuator

Figure 13. Testing the BLDC axial motor option: (a) test stand and (b) basic test result

Figure 14(a) shows the experimental set-up for tests with radial BLDC motor. The tests have confirmed the FEM analyses, as the controller does not need to compensate any axial forces induced by the motor. As shown in Fig.14(b), using the radial motor, the current in the electromagnetic actuator of the AMB-EPUSP even decreases, from 0.2 to −0.06A while the motor speed changes from 0 to 600 RPM.

(a) Set-up

(b) Current in the actuator

Figure14. Testing the BLDC radial motor option

6. CONCLUSIONS

Table 1 shows a summary of the BLDC motor options characteristics, based on the preliminary tests, where the best characteristics are highlighted. The FEM analyses corroborate on the recommendation of the radial BLDC motor option as the best choice to drive the VAD with AMB-EPUSP magnetic suspension, because it magnetic suspension does not need to compensate any axial forces generated by the motor. However, as shown in Fig. 3, the radial BLDC motor assembling should cause some mechanical interference with the VAD outlet, which may require a more complex VAD design.

Table 1. Characteristics of the AMB-EPUSP magnetic suspension versus BLDC motor option

Characteristics	Axial option	Radial option
Windings	**Less copper**	More copper
Windings room	Small	**Not critical**
Torque	Good	**Better**
Axial forces	Critical	**Not relevant**
Radial forces	**Not relevant**	**Not relevant**
Gap	The axial force changes the gap	**No problem**
Change motor gap	**Easy**	Requires motor redesign
Inlet interference	**No mechanical interference**	**No mechanical interference**
Outlet interference	**No mechanical interference**	Yes
Suspension affected	Yes	**No**
Suspension influence	The gap changes increases with the rotor speed	**Minimal influence**
PID Controller	May require redesign	**Satisfactory**
Best choice	No	**Yes**

The initial tests confirm that the axial force, generated by the axial BLDC motor option, induces a strong instability on the AMB-EPUSP magnetic suspension, demanding high current to control the rotor position. The preliminary data indicate the current controller design will not be able to guarantee the magnetic bearing stability with axial motor on higher velocities, but future tests will confirm it or not.

On any case, additional study is recommend to evaluate the rotor dynamic instability of the AMB-EPUSP magnetic suspension with the rotor surrounded by "blood", since the liquid environment should absorb the oscillation energy (Vance *et al*, 2010) and minimize the restriction due to the magnetic suspension instability on frequencies below 5000 RPM.

7. ACKNOWLEDGEMENTS

8. REFERENCES

Aboulnaga, A.A. and Emadi, A.. "Design of high performance linear brushless DC motor with ironless core". The 4th International Power Electronics and Motion Control Conference, IEEE, Volume 2, 502-507, 2004.

Andrade, A., Biscegli, J., Dinkhuysen, J., Sousa, J.E., Ohashi, Y., Hemmings, S., Glueck, J., Kawahito, K. and Nose, Y. (1996), "Characteristics of a Blood Pump Combining the Centrifugal and Axial Pumping Principles: The Spiral Pump". Artificial Organs, Vol.20(6), 605-612.

Asama, J., Fukao, T., Chiba, A., Rahman, A. and Oiwa, T.. "A new design for a Compact Centrifugal Blood Pump with a Magnetically Levitated Rotor". ASAIO Journal, vol. 50, no 6, 550-556p, 2004.

Berne, R.M. and Levy, M.N.. "The Cardiac Pump. Cardiovascular Physiology", Cap.3, Mosby Inc., 8a edição, 68-79p, 2001.

Challa, S.K.. "Comparative Study of Axial Flux Permanent Magnet Brushless DC Motor Operating with the Winding Connected in Single-Phase and Two-Phase System". 162p. Tese (Mestrado) – Agricultural and Mechanical College, Louisiana State University, Louisiana, 2006.

Horikawa, O., Andrade, A.J.P; Silva, I. and Bock, E.G.P.. "Magnetic Suspension of the Rotor of a Ventricular Assist Device of Mixed Flow Type". Artificial Organs, Vol.32(4), 334-341p, 2008.

Legendre, D., Antunes, P., Bock, E., Andrade, A., Biscegli, J. and Ortiz, J.. "Computational Fluid Dynamics Investigation of a Centrifugal Blood Pump". Artificial Organs, Vol.32(4), 342-348p, 2008.

Ooshima, M.. "Analyses of Rotational Torque and Suspension Force in a Permanent Magnet Synchronous Bearingless Motor with Short-pitch Winding". Power Engineering Society General Meeting, IEEE, 7p, 2007.

Silva, I. and Horikawa, O.. "An 1-DOF Controlled Attraction Type Magnetic Bearing", IEEE Transaction on Industry Applications, Vol.36 (4), 1138, 2000.

Silva, I.. "Mancais Magnéticos Híbridos do tipo atração com Controle Uniaxial". 2005. 162p. Tese (Doutorado) – Escola Politécnica, Universidade de São Paulo, São Paulo, 2005.

Vance, J., Zeidan, F. and Murphy, B.. "Machinery Vibration and Rotordynamics". 1.ed. John Wiley & Sons, Inc. 2010. 419p

9. RESPONSIBILITY NOTICE

The authors are the only responsible for the printed material included in this paper.